

Performance analysis of TBM excavation parameters related to small-diameter horizontal and inclined tunnels

Original

Performance analysis of TBM excavation parameters related to small-diameter horizontal and inclined tunnels / Cardu, Marilena; Todaro, Carmine; Farzay, Oveis; Di Giovanni, Alfio; Saltarin, Simone. - ELETTRONICO. - (2024), pp. 1669-1674. (ITA-AITES WORLD TUNNEL CONGRESS 2024 (WTC 2024) SHENZHEN, CHINA 19-25 April 2024).

Availability:

This version is available at: 11583/2988886 since: 2024-05-21T15:07:20Z

Publisher:

Taylor & Francis

Published

DOI:

Terms of use:

This article is made available under terms and conditions as specified in the corresponding bibliographic description in the repository

Publisher copyright

Taylor and Francis postprint/Author's Accepted Manuscript con licenza CC by-nc-nd

This is an Accepted Manuscript version of the following article: Performance analysis of TBM excavation parameters related to small-diameter horizontal and inclined tunnels / Cardu, Marilena; Todaro, Carmine; Farzay, Oveis; Di Giovanni, Alfio; Saltarin, Simone. - ELETTRONICO. - (2024), pp. 1669-1674. (ITA-AITES WORLD TUNNEL CONGRESS 2024 (WTC 2024) SHENZHEN, CHINA 19-25 April 2024).. It is deposited under

(Article begins on next page)

Steady-State Analysis of Switching Power Converters via Augmented Time-Invariant Equivalents

Riccardo Trinchero, *Student Member, IEEE*, Igor S. Stievano, *Senior Member, IEEE*,
Flavio G. Canavero, *Fellow, IEEE*

Abstract—This letter addresses the simulation of the steady-state response of switching power converters. The proposed approach is based on the interpretation of the voltage and current variables of a periodically switched linear circuit in terms of a series expansion and on the generation of augmented time-invariant constitutive relations of the circuit elements. The circuit solution is obtained from an augmented time-invariant nodal equation generated from topological information and circuit inspection only. The feasibility and strength of the approach are demonstrated on a DC-DC boost converter.

I. INTRODUCTION

Switched-mode power converters represent a class of well-known circuits massively used in a wide range of applications for supplying energy to electrical and electronic equipment and appliances. These circuits are inherently time-varying systems with a complex time-domain behavior characterized by the superposition of slow and fast dynamics, the latter arising from the internal periodic activity of the switching devices.

The above features demand for the availability of effective simulation techniques for circuit analysis in the early design phase, with specific emphasis on the prediction of both the frequency- and time-domain behavior of the converter. Numerical simulation is used for the systematic assessment of possible alternative design scenarios and control strategies or the selection of the optimal filtering technique aimed at suppressing the unavoidable periodic disturbances feeding the power distribution system (see e.g., [1], [2], [3], [4]).

In this framework, a number of techniques have already been developed and are currently available in the literature. Classical methods such as those based on state-space averaging or possible enhancements provide an effective solution that is widely adopted by designers [5], [6], [7], [8], [9], [10], [11]. The aforementioned tools, provide a fast and effective simulation of the average response of the converters. To fully characterize the high-frequency behavior of circuit responses, further improvements or other techniques based on the general theory of periodically switched linear (PSL) circuits and systems can be used. Without loss of generality, the readers

should refer to [12], [13], [14], [15] for a selection of state-of-the-art contributions in this field. The above methods, that enhance the basic mathematical tool for the analysis of switching circuits or time-varying systems with periodic behavior, share the common limitation that the formulation and development are in general cumbersome. Hence, they demand for improvements aimed at lowering the technical barrier and facilitating the use of these methods for practical and realistic designs, with a large number of components, via a simple simulation strategy.

Therefore, the aim of this paper is to provide a solution that reduces the mathematical complexity and allows to generate a simulation stamp describing the circuit components, including the switches, by means of augmented time-invariant representations. As a result, the steady-state response of a PSL circuit is carried out via the standard solution of an augmented time-invariant nodal equation generated from circuit inspection only. As an additional benefit with respect to most of the state-of-the-art methods, the proposed technique handles an arbitrary number of switching devices within an automatic simulation flow and without introducing additional numerical overhead and complexity. The approach is illustrated and validated on a realistic switching power converter.

II. SIMULATION STRATEGY

This Section briefly summarizes the proposed procedure for the case of an arbitrarily complex PSL circuit consisting of the interconnection of linear time-invariant (LTI) elements and switches.

For the sake of illustration and concreteness, the letter is focused on the DC-DC boost converter shown in Fig. 1. This example offers a representative test case that allows to stress the benefits of the proposed methodology. In the schematic of Fig. 1, the MOS device is driven by a square wave with a switching frequency $f_c = 10$ kHz and a suitable duty-cycle D , that is provided by an analog feedback network as a function of v_C and i_L .

The mathematical framework of linear periodic time-varying systems suggests to approximate the steady-state behavior of PSL circuits to cisoidal excitations at angular frequency ω_0 in terms of a truncated harmonic expansion (e.g., see [12], [16] and references therein). E.g., for the current $i_L(t)$ in the schematic of Fig. 1, its corresponding Fourier series writes:

Manuscript received February 27, 2014; revised May 2, 2014; accepted May 2, 2014. DOI 10.1109/TPEL.2014.2322259, IEEE Transactions on Power Electronics.

R. Trinchero, I.S. Stievano and F. G. Canavero are with the Department of Electronics and Telecommunications, Politecnico di Torino, Corso Duca degli Abruzzi, 24, 10129, Torino, Italy, e-mail: {riccardo.trinchero, igor.stievano, flavio.canavero}@polito.it.

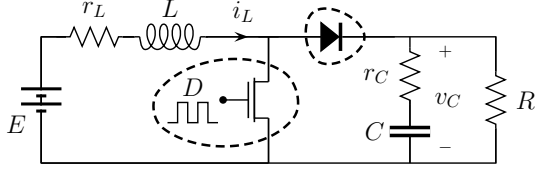


Figure 1. Example test case: DC-DC boost converter with its relevant electrical variables. The circuit elements take the following values: $E = 20$ V, $r_L = 1$ m Ω , $L = 5$ mH, $r_C = 5$ m Ω , $C = 10$ μ F, $R = 20$ Ω .

$$I_L(\omega) \approx \sum_{n=-N}^{+N} I_{L,n} \delta(\omega - n\omega_c - \omega_0), \quad (1)$$

where $\omega_c = 2\pi f_c$ is the switching angular frequency and $I_{L,n}$ are the Fourier coefficients of the n -th harmonic of the current i_L . The same approximation holds for all the other voltage and current variables. It is relevant to remark that this is the underlying interpretation similar to other tools like the so-called harmonic balance, that is based on the Fourier expansion of the steady-state responses of a possibly nonlinear or periodically-varying system (e.g., see [12], [17]).

In this letter, the coefficients of the advocated expansion are interpreted as new variables of an augmented circuit where the characteristics of both the time-varying switches and the standard LTI elements are recast in terms of new time-invariant constitutive relations. The above interpretation allows to predict the steady-state response of a PSL circuit via the solution of a LTI augmented nodal equation via simple linear inversion. Summarizing, the proposed simulation method can be decomposed into the following two steps: (i) generate augmented LTI characteristics of all the circuit elements and (ii) obtain the steady-state solution of the original circuit in terms of the solution of an augmented LTI nodal equation. The method is described in details and applied to the example boost circuit of Fig. 1.

III. AUGMENTED CHARACTERISTICS

This Section addresses the generation of the augmented characteristics of the basic circuit components used in the schematic of Fig. 1. For notational convenience, a generic two-terminal element with the associated voltage $v(t)$ current $i(t)$ variables defined with passive sign convention is assumed. The electrical variables are represented by means of their corresponding Fourier transforms and are approximated by means of a truncated series of delta functions, following the same notation of (1) (e.g., $V(\omega) \approx \sum_{n=-N}^{+N} V_n \delta(\omega - n\omega_c - \omega_0)$).

For the case of a simple LTI resistor with characteristic $v = Ri$, the relation between its current and voltage harmonics turns out to be frequency independent and writes:

$$I_n = V_n/R, \quad n = -N, \dots, 0, \dots, N. \quad (2)$$

For the case of dynamic LTI elements, such as the capacitor with $i = Cdv/dt$, the corresponding constitutive relation becomes:

$$I_n = j(\omega_0 + n\omega_c)CV_n, \quad n = -N, \dots, 0, \dots, N, \quad (3)$$

and similarly for an inductor.

When dealing with a switch, the computation requires additional efforts instead. However, the derivation is only carried out once. The generic switch is assumed to be described by the two-terminal element of Fig. 2 that consists of the series connection of an ideal switching element S_k and of a finite series resistance R_k . The above element can be considered as the basic switching block describing the behavior of both the MOS transistor and the diode of Fig. 1 that change their state in opposition of phase during normal operation. The switch S_k is characterized by a periodic switching activity between the open and the close position with a characteristic period T and frequency $f_c = 1/T$ according to the illustrative plot in the Fig. 2.

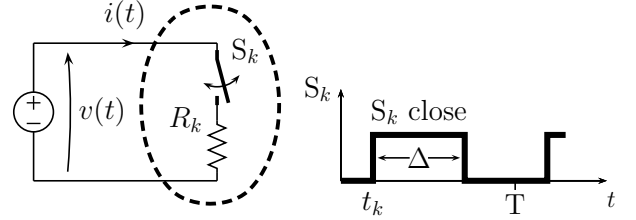


Figure 2. Example circuit for the generation of an augmented time-invariant equivalent of the switch ($\Delta = D_k T$).

In the schematic of Fig. 2, the PSL element is driven by an ideal voltage source to allow the computation of its generalized admittance representation, i.e., the constitutive relation involving the port voltage $v(t)$ and the current $i(t)$ as the input and output variables, respectively.

Since the switching block does not include dynamical elements, the port current $i(t)$ can be interpreted as the juxtaposition in time of the current response computed from the analysis of the circuit of Fig. 2 at each operating state of the switch (i.e., open and close).

To simplify the derivation, the generic m -th component of the expansion of the voltage variable is considered only, i.e. $V_m(\omega) = V_m \delta(\omega - m\omega_c - \omega_0)$ or equivalently in the time-domain $v(t) = (V_m/2\pi) \exp(j(m\omega_c + \omega_0)t)$. Hence, the current $i(t)$ writes:

$$i(t) = v(t)G_k \sum_{q=-\infty}^{+\infty} \Pi_{D_k}(t - t_k - qT) \quad (4)$$

where, $G_k = 1/R_k$ and Π is the window function defined by:

$$\Pi_{D_k}(t - t_0) = \begin{cases} 1 & t_0 \leq t \leq D_k T + t_0 \\ 0 & \text{otherwise} \end{cases} \quad (5)$$

The direct application of the Fourier transform to (4) leads, via a relatively long but straightforward manipulation, to:

$$\begin{aligned} I(\omega) &\approx \sum_{n=-N}^{+N} I_n \delta(\omega - n\omega_c - \omega_0) \\ &= \sum_{q=-N}^{+N} Y_{q,k} V_m \delta(\omega - (m+q)\omega_c - \omega_0) \end{aligned} \quad (6)$$

for $|m + q| \leq N$, where

$$Y_{q,k} = f_c G_k \int_{t_k}^{t_k + D_k T} 1 \exp(-jq\omega_c t) dt \\ = f_c G_k \frac{\exp(-jq\omega_c t_k) - \exp(-jq\omega_c(t_k + D_k T))}{jq\omega_c}. \quad (7)$$

In this example, the coefficients $Y_{q,k}$ do not depend on the variable ω_0 since the circuit in each operating state is resistive and its solution involves instantaneous relations only. It is worth noticing that the time-domain response of the system is readily obtained from (6) by replacing the delta functions $\delta(\omega - n\omega_c - \omega_0)$ with the complex exponential terms $\exp(j(\omega_0 + n\omega_c)t)$.

When the voltage excitation $v(t)$ includes all the harmonics, the constitutive relation of the basic switching element of Fig. 2 can be proven to be recast as:

$$\begin{bmatrix} I_{-N} \\ \vdots \\ I_0 \\ \vdots \\ I_N \end{bmatrix} = \begin{bmatrix} Y_{0,k} & Y_{-1,k} & \cdots & \cdots & Y_{-2N,k} \\ Y_{1,k} & Y_{0,k} & \cdots & \cdots & \vdots \\ \vdots & \vdots & \ddots & \vdots & \vdots \\ \vdots & \vdots & \vdots & \ddots & Y_{-1,k} \\ Y_{2N,k} & \cdots & \cdots & Y_{1,k} & Y_{0,k} \end{bmatrix} \begin{bmatrix} V_{-N} \\ \vdots \\ V_0 \\ \vdots \\ V_N \end{bmatrix} \quad (8)$$

where the voltage and current variables $V(\omega)$ and $I(\omega)$ are replaced by the vectors $\mathbf{V} = [V_{-N}, \dots, V_0, \dots, V_N]^T$ and $\mathbf{I} = [I_{-N}, \dots, I_0, \dots, I_N]^T$. The above vectors, that have dimension $(2N + 1) \times 1$, are filled in by the harmonic coefficients defining the steady-state response of the corresponding variables and play the role of the new port variables of an augmented circuit element.

Equation (8), that turns out to be an LTI representation of the PSL element, can be written in a more compact form as

$$\mathbf{I} = \mathbf{Y}_k \mathbf{V} \quad (9)$$

where \mathbf{Y}_k is the $(2N + 1) \times (2N + 1)$ matrix in (8). The above equation also highlights that the switch leads to a fully coupled augmented characteristic involving the combination of all the different harmonics. On the contrary, the companion characteristics of the LTI components turn out to be defined by diagonal matrices.

It is important to remark that the matrix entries $Y_{q,k}$ are coefficients defined by the closed-form analytical formula (7) and that can be easily computed from the information of the switching operation of the k th switch in the circuit only. Also, the stamp (9), that is computed once, can be used to approximate the behavior of any binary switching device in a PSL circuit.

IV. AUGMENTED MNA AND RESULTS

This Section specializes the classical modified nodal analysis (MNA) tool for circuit analysis to the case of circuits composed by linear time-invariant elements and switches. For conciseness, the derivation is based on the example circuit of

Fig. 3, that has the same topology of the boost circuit of Fig. 1 where both the MOS transistor and the diode are replaced by the gray two-terminal switching elements labeled as Y_1 and Y_2 respectively. For notational convenience, the other circuit components are identified by their admittances in the framework of phasor analysis for the solution of circuits operating in the sinusoidal steady-state. Also, the nodal unknowns, i.e., the voltages $V_1(\omega)$, $V_2(\omega)$, $V_3(\omega)$ and $V_4(\omega)$ and the current through the inductor $I_L(\omega)$ are the Fourier transform of their corresponding steady-state circuit responses. Similarly, $E(\omega)$ is the Fourier transform of the time domain excitation signal (both constant and periodic signals are covered by this method). The above interpretation is introduced to facilitate the derivation of the MNA equations governing PSL circuits with the switches described by the augmented characteristics introduced in the previous Section.

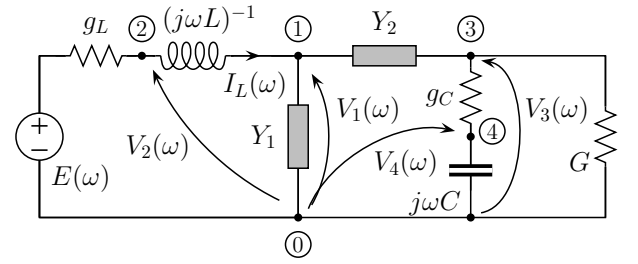


Figure 3. Example circuit used for the generation of an augmented time-invariant MNA equation of the boost converter of Fig. 1 (the gray two-terminal elements Y_1 and Y_2 represents the switches). The other LTI components are identified by their corresponding frequency-domain admittances.

The discussion starts with the well-known stamp arising from the analysis of the schematic of Fig. 3 where Y_1 and Y_2 are simple LTI admittances (e.g., $Y_{1,2} = j\omega C_{1,2}$). In this case, the MNA equation in matrix form writes:

$$\begin{bmatrix} Y_1 + Y_2 & 0 & -Y_2 & 0 & -1 \\ 0 & g_L & 0 & 0 & 1 \\ -Y_2 & 0 & Y_2 + g_C + G & -g_C & 0 \\ 0 & 0 & -g_C & g_C + j\omega C & 0 \\ -1 & 1 & 0 & 0 & -Z_L \end{bmatrix} \begin{bmatrix} V_1 \\ V_2 \\ V_3 \\ V_4 \\ I_L \end{bmatrix} = \begin{bmatrix} 0 \\ g_L E \\ 0 \\ 0 \\ 0 \end{bmatrix} \quad (10)$$

When the impedances Y_1 and Y_2 are replaced by two switches like the one in Fig. 2, the nodal variables need to be replaced by the corresponding vectors \mathbf{V}_1 , \mathbf{V}_2 , \mathbf{V}_3 , \mathbf{V}_4 and \mathbf{I}_L that collect the coefficients of the harmonic series expansion of the unknowns. The characteristic of all the circuit components must be replaced accordingly. As an example, the forth row of (10), $g_C(V_4 - V_3) + j\omega C V_4 = 0$, is replaced by the augmented equation (12), that in compact matrix form writes:

$$g_C \mathbf{1}(\mathbf{V}_4 - \mathbf{V}_3) + \mathbf{Y}_C \mathbf{V}_4 = \mathbf{0}. \quad (11)$$

Summarizing, the augmented characteristics of the two switches defined by (9) and the companion relations that can be readily obtained for the classical LTI elements allow to replace the original MNA equation with (13), where the role and definition of the new entries of the matrix and

variables comes from the explicit expansion of (12) and the source term $E(\omega) = (E/2\pi)\delta(\omega)$ is replaced by the vector $E=[0, \dots, E, \dots, 0]^T$.

It is worth to remark that equation (13) turns out to be $(2N+1)$ times larger than the corresponding MNA equation of a circuit with the switching elements replaced by linear-time invariant impedances. However, the proposed extended matrix, that belongs to the same class of (10), can be readily solved via simple linear inversion. What is more important, the steady-state response of the the PSL circuit can be computed via equations like (1) by re-interpreting the coefficients of the new voltage and current unknowns.

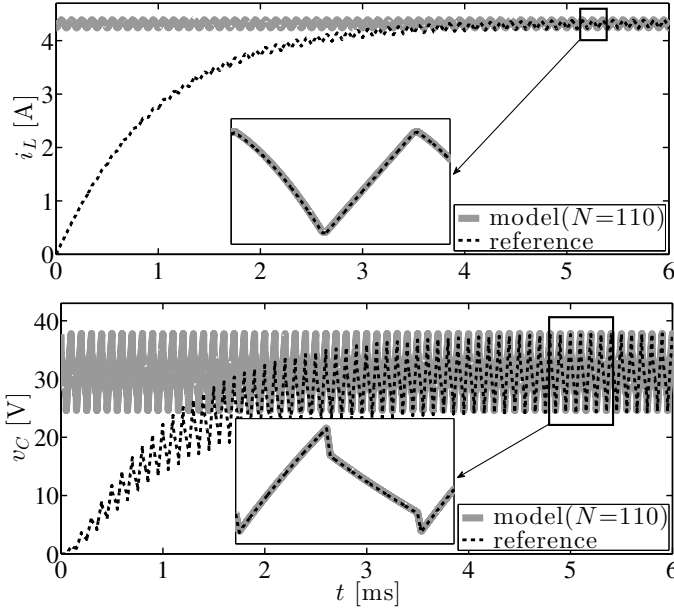


Figure 4. Time-domain response of the current $i_L(t)$ and voltage $v_C(t)$ of the circuit in Fig. 1 ($D = 50\%$). Dashed black: reference; Solid gray: prediction (13) and order expansion $N = 110$.

To validate the method, Fig. 4 collects the comparison between the reference and the predicted time-domain responses of the inductor current $i_L(t)$ and the output voltage $v_C(t)$. The reference responses of the circuit are computed by means of Matlab[®] and the standard ordinary differential equation integration routines. The curves in the figure highlight the good accuracy of the proposed solution in reproducing the steady-state response of the boost circuit via (13) without the inclusion of the initial transient observed in the reference curve.

It is important to remark that in this comparison the two switches describing the MOS and the diode are assumed to have a non ideal behavior, with an overlapping of 1% of the switching period T in which they are both closed. This is a parasitic condition occurring in a real power converter that explains the spikes in the voltage response (see the bottom panel of Fig. 4). Owing to this, the expansion order is set to a sufficiently large number (i.e., $N = 110$) to allow for the inclusion of the high frequency components of the responses in the proposed steady-state analysis. As far as the accuracy and efficiency is concerned, a speed-up of $177\times$ (0.13 s) and a mean square error-computed from the difference between

the reference and the predicted responses of $< 0.25\%$ only is achieved.

V. CONCLUSIONS

This letter addressed the simulation of the steady-state response of a switched-mode power converter. The proposed solution extends the results of previously published papers in this field and is based on the generation of an augmented time-invariant MNA equation governing the circuit behavior. A topological approach is considered, with emphasis on an intuitive physical based interpretation of the switching elements in the network. The proposed solution has been proven to offer a modular approach to circuit analysis, leading to accurate results with good simulation speed-ups. The present implementation requires a dedicated code to carry out the numerical simulation (as an example, the results collected in this letter are based on Matlab[®]). It is also worth mentioning that a high-frequency characterization of switching circuits unavoidably demands for a relatively large number of harmonics to be included in the model.

REFERENCES

- [1] I. Cadirci, B. Saka, Y. Eristiren, "Practical EMI-filter-design procedure for high-power high-frequency SMPS according to MIL-STD 461," IEE Proceedings – Electric Power Applications, Vol. 152, No. 4, pp. 775–782, Jul. 8, 2005.
- [2] L. Corradini, P. Mattavelli, "Modeling of Multisampled Pulse Width Modulators for Digitally Controlled DC–DC Converters", IEEE Trans. on Power Electronics, Vol. 23, No. 4, pp. 1839–1847, Jul. 2008.
- [3] V. Tarateeraseth, S. Kye Yak, F.G. Canavero, R.W. Chang, "Systematic Electromagnetic Interference Filter Design Based on Information From In-Circuit Impedance Measurements", IEEE Trans. on Electromagnetic Compatibility, Vol. 52, No. 3, pp. 588–598, Aug. 2010.
- [4] V. Tarateeraseth, I.A. Maio, F.G. Canavero, "Assessment of Equivalent Noise Source Approach for EMI Simulations of Boost Converter.", Proc. of the 20th Int. Zurich Symposium on EMC, pp. 353–356, Jan. 2009.
- [5] R. Ericson, D. Maksimovic, "Fundamentals of Power Electronics", Kluwer Academic Publisher, 2001.
- [6] A. Davoudi, J. Jatskevich, T. De Rybel, "Numerical state-space average-value modeling of PWM DC-DC converters operating in DCM and CCM", IEEE Trans. on Power Electronics, Vol. 21, No. 4, pp. 1003–1012, Jul. 2006.
- [7] K. Gorecki, J. Zarebski, "The Method of a Fast Electrothermal Transient Analysis of Single-Inductance DC-DC Converters", IEEE Trans. on Power Electronics, Vol. 27, No. 9, pp. 4005–4012, Sept. 2012.
- [8] T. Pavlovic, T. Bjazic, Z. Ban, "Simplified Averaged Models of DC-DC Power Converters Suitable for Controller Design and Microgrid Simulation", IEEE Trans. on Power Electronics, Vol. 28, No. 7, pp. 3266–3275, July 2013.
- [9] S. Ben-Yaakov, "Behavioral Average Modeling and Equivalent Circuit Simulation of Switched Capacitors Converters", IEEE Tans. on Power Electronics, Vol. 27, No. 2, pp. 632–636, Feb. 2012.
- [10] Q. Hengsi, J. W. Kimball, "Generalized Average Modeling of Dual Active Bridge DC-DC Converter", IEEE Trans. on Power Electronics, Vol. 27, No. 4, pp. 2078–2084, April 2012.
- [11] R. Priewasser, M. Agostinelli, C. Unterrieder, S. Marsili, M. Huemer, "Modeling, Control, and Implementation of DC-DC Converters for Variable Frequency Operation", IEEE Trans. on Power Electronics, Vol. 29, No. 1, pp. 287–301, Jan. 2014.
- [12] H. Sandberg, E. Mollerstedt, Bernhardsson, "Frequency-domain analysis of linear time-periodic systems", IEEE Trans. on Automatic Control, Vol. 50, No. 12, pp. 1971–1983, Dec. 2005.
- [13] H. Behjati, L. Niu, A. Davoudi, P. L. Chapman, "Alternative Time-Invariant Multi-Frequency Modeling of PWM DC-DC Converters", IEEE Trans. on Circuits and Systems I: Regular Papers, Vol. 60, No. 11, pp. 3069–3079, Nov. 2013.
- [14] J. A. Alvarez Martin, J. R. Melgoza, J. J. Rincon Pasaye, "Exact steady state analysis in power converters using Floquet decomposition.", Proc. of the North American Power Symposium, pp. 1–7, Aug. 2011.

$$\begin{bmatrix} g_C & 0 & 0 \\ 0 & \ddots & 0 \\ 0 & 0 & g_C \end{bmatrix} \left(\begin{bmatrix} V_{4,-N} \\ \vdots \\ V_{4,N} \end{bmatrix} - \begin{bmatrix} V_{3,-N} \\ \vdots \\ V_{3,N} \end{bmatrix} \right) + \begin{bmatrix} j(\omega_0 - N\omega_c)C & 0 & 0 \\ 0 & \ddots & 0 \\ 0 & 0 & j(\omega_0 + N\omega_c)C \end{bmatrix} \begin{bmatrix} V_{4,-N} \\ \vdots \\ V_{4,N} \end{bmatrix} = \begin{bmatrix} 0 \\ \vdots \\ 0 \end{bmatrix} \quad (12)$$

$$\left[\begin{array}{c|c|c|c|c} \mathbf{Y}_1 + \mathbf{Y}_2 & \mathbf{0} & -\mathbf{Y}_2 & \mathbf{0} & -\mathbf{1} \\ \hline \mathbf{0} & g_L \mathbf{1} & \mathbf{0} & \mathbf{0} & \mathbf{1} \\ \hline -\mathbf{Y}_2 & \mathbf{0} & \mathbf{Y}_2 + (g_C + G)\mathbf{1} & -g_C \mathbf{1} & \mathbf{0} \\ \hline \mathbf{0} & \mathbf{0} & -g_C \mathbf{1} & g_C \mathbf{1} + \mathbf{Y}_C & \mathbf{0} \\ \hline -\mathbf{1} & \mathbf{1} & \mathbf{0} & \mathbf{0} & -\mathbf{Z}_L \end{array} \right] \begin{bmatrix} \mathbf{V}_1 \\ \mathbf{V}_2 \\ \mathbf{V}_3 \\ \mathbf{V}_4 \\ \mathbf{I}_L \end{bmatrix} = \begin{bmatrix} \mathbf{0} \\ g_L \mathbf{E} \\ \mathbf{0} \\ \mathbf{0} \\ \mathbf{0} \end{bmatrix} \quad (13)$$

- [15] J. Kovar, Z. Kolka, D. Biolek, "Comparison of averaging and harmonic balance methods for switched DC-DC converters.", in *Proc. of 17th Int. Conf. on Mixed Design of ICs and Systems*, pp. 402–407, June 2010.
- [16] T.A.C.M. Claasen, W. F. G. Mecklenbrauker, "On stationary linear time-varying systems", *IEEE Trans. on Circuits and Systems*, Vol. 29, No. 3, pp. 169–184, Mar. 1982.
- [17] J. Roychowdhury, "Reduced-order modeling of time-varying systems", *IEEE Transactions on Circuits and Systems II: Analog and Digital Signal Processing*, Vol. 46, No. 10, pp. 1273–1288, Oct 1999.